nature structural biology

The structure of BtuB with bound colicin E3 R-domain implies a translocon

Genji Kurisu[1,2,6], Stanislav D Zakharov[1,3,6], Mariya V Zhalnina[1,6], Sufiya Bano[1], Veronika Y Eroukova[4], Tatiana I Rokitskaya[4], Yuri N Antonenko[4], Michael C Wiener[5] & William A Cramer[1]

Cellular import of colicin E3 is initiated by the *Escherichia coli* outer membrane cobalamin transporter, BtuB. The 135-residue 100-Å coiled-coil receptor-binding domain (R135) of colicin E3 forms a 1:1 complex with BtuB whose structure at a resolution of 2.75 Å is reported. Binding of R135 to the BtuB extracellular surface ($\Delta G° = -12$ kcal mol^{-1}) is mediated by 27 residues of R135 near the coiled-coil apex. Formation of the R135–BtuB complex results in unfolding of R135 N- and C-terminal ends, inferred to be important for unfolding of the colicin T-domain. Small conformational changes occur in the BtuB cork and barrel domains but are insufficient to form a translocation channel. The absence of a channel and the peripheral binding of R135 imply that BtuB serves to bind the colicin, and that the coiled-coil delivers the colicin to a neighboring outer membrane protein for translocation, thus forming a colicin translocon. The translocator was concluded to be OmpF from the occlusion of OmpF channels by colicin E3.

Protein import in organelles and secretion from bacteria is carried out by receptor complexes ('translocons') that have been described structurally[1–4]. However, neither a high-resolution structure nor evidence of structure changes caused by formation of the complex between receptor and translocating protein has been provided for any receptor component in these translocons. The receptor and helper protein system that translocates cytotoxic colicins across the cell envelope can provide information about the structural basis of protein import. Colicins are translocated into the cytoplasmic membrane or through the membrane to the cytoplasm by a sequence of transfer steps carried out by a protein import network that spans the *E. coli* cell envelope[5,6]. The initial step is binding to one or more receptor(s) in the outer membrane. In contrast to the description of protein translocation in the organelle and bacterial systems enumerated above, the receptor for colicins in the outer membrane is generally viewed as involving a single outer membrane protein[5,7,8], although the possible involvement of two receptors has been noted[6,9]. The present study reports a new structure of the complex of the integral outer membrane receptor, BtuB, andthe receptor-binding domain of a colicin; this structure provides insights into the structural basis of receptor-mediated colicin translocation across the outer membrane and the issue of the translocon.

Colicins and phages are 'opportunistic cargo' for receptors in the outer membrane whose physiological function is to bind and transport metabolites (such as metals, sugars and vitamins). Colicin E3, used in the present study, is a ribosomal endoribonuclease[10]. A prominent feature of the colicin E3 structure is an elongate (100 Å) helical coiled-coil receptor-binding domain (**Fig. 1a**). Residues 316–448 of the coiled coil form an antiparallel 'Alacoil'[11] whose helical arms containing residues 316–378 and 386–448 are connected by a seven-residue loop[10]. It was proposed that the function of a similar extended coiled coil in the structure of colicin Ia is to span the periplasmic space between the inner and outer membranes[12]. We propose a different function for the elongate coiled coil of colicin E3.

The *E. coli* outer membrane receptor(s) used by the E-group colicins, colicin A and phage BF23 is the 594-residue *E. coli* outer-membrane cobalamin translocator BtuB[13,14]. Crystal structures of BtuB have been obtained for (i) apo cobalamin (ii) Ca^{2+} and (iii) Ca^{2+}-cobalamin forms of BtuB[15]. The 22-strand antiparallel β-barrel motif found for BtuB has been described for the Fe siderophore–binding FepA[16] and FhuA[17], which are the receptors for colicins B and M, respectively, and the ferric citrate–binding FecA[18]. All of these outer-membrane receptor proteins contain an N-terminal globular domain of 130–150 residues, 132 residues in BtuB, which folds into the lumen of the barrel like a channel 'cork.' This cork occludes the lumen of the β-barrel and shares an extensive binding surface with the inside of the barrel[16,17] so that it is difficult to envision how these receptors translocate substrates without some displacement of the cork. The problem of bypassing the cork domain is even more formidable for translocation of a colicin polypeptide. To obtain insight into the mechanism of translocation of colicin E3 across the outer membrane, BtuB was cocrystallized in detergent in complex with the isolated coiled-coil receptor-binding domain, R135, of colicin E3.

[1]Department of Biological Sciences, Purdue University, Lilly Hall of Life Sciences, 915 W. State St., West Lafayette, Indiana 47907-1392, USA. [2]Institute for Protein Research, Osaka University, Suita, Osaka 565-0871, Japan. [3]Institute of Basic Biological Problems, Russian Academy of Sciences, Puschino, Russia 142290. [4]Belozersky Institute, Moscow State University, Moscow, Russia 11999. [5]Department of Molecular Physiology and Biological Physics, University of Virginia, Charlottesville, Virginia 22908, USA. [6]These authors contributed equally to this work. Correspondence should be addressed to W.A.C. (wac@bilbo.bio.purdue.edu).

Published online 5 October 2003; doi:10.1038/nsb997

RESULTS

Structure of BtuB–R135 complex

A 135-residue receptor-binding domain (R135, Thr313–Glu447) of colicin E3 was cloned and expressed as a His-tagged protein (**Fig. 1a**). The dissociation constant for R135 binding to BtuB, determined by biosensor assay, and qualitatively confirmed by microbiological spot tests[19], is $K_d = 0.9 \pm 0.2$ nM ($k_a = 4.5 \pm 0.1 \times 10^5$ s^{-1} M^{-1}; $k_d = 4.1 \pm 0.5 \times 10^{-4}$ s^{-1}) at pH 8, 0.1 M ionic strength. This corresponds to a free energy of binding of R135 of approximately –12 kcal mol^{-1}. R135 competes efficiently for BtuB with colicin E3 in the spot test protection assay, implying that its binding affinity for BtuB is comparable to that of colicin E3. The secondary structure of the isolated R135 peptide was highly (92%) α-helical. Because of the predominantly β-strand structure of BtuB[15], it was possible using far-UV circular dichroism (CD) to measure the changes in helical content of R135, caused by binding to BtuB (**Fig. 2**). Upon complex formation, the helical content of R135 decreased by 12 ± 5%.

Conformational changes of R135

Crystals of the 1:1 complex of BtuB and R135 diffracted to 2.75 Å (**Table 1** and see **Supplementary Fig. 1** online). The structure was solved by molecular replacement using the apo BtuB structure[15]. It shows BtuB in complex with the 116 ordered residues of R135 in a coiled-coil conformation (**Fig. 1b**). Nineteen residues of R135, the N-terminal ten residues, Thr313–Asn322 and the C-terminal nine residues, Lys439–Glu447, are disordered and not resolved in the structure. The disordered regions of R135 induced by binding to BtuB account for 14% of the structure, which agrees with determination by difference far-UV CD (**Fig. 2**). The crystal contacts in the unit cell were formed mainly by Gln341 and Glu342 from R135. Thus, they do not affect the extent of the unfolding of R135 upon binding to BtuB. The consistent values of the extent of unfolding show that the N and C termini, with exception of C-terminal $Glu(His)_6$, are in a helical conformation in isolated R135. This is consistent with NMR data on the folded state of the R76 peptide from the homologous R-domain of colicin E9 (ref. 20), which inhibits growth of a vitamin B_{12}–dependent *E. coli* strain[21]. The systematic development of this disorder along the coiled coil, induced by receptor binding, can be seen in the Cα displacement of the residues of the bound R135 relative to those in colicin E3 (ref. 10). The Cα displacement increases with increasing distance from the tip region of R135 involved in binding (**Fig. 1c**). The displacements of the last observable residues at the N and C termini of R135 are 3.5 and 6 Å for Tyr323 and Lys438, respectively. As discussed below, the function of this unfolding, which is presumably driven by the –12 kcal mol^{-1} of binding energy, may be to trigger unfolding of the colicin that is necessary for its passage across the outer membrane. This binding energy is sufficient to dissociate the T-domain from its interface with immunity protein (Imm) (**Fig. 1a**), if it can be transduced, as the binding energy between these two domains is no more than about –2.7 kcal mol^{-1}, which is 15% of the binding energy for Imm (2.7 kcal mol^{-1} out of a total of 19 kcal mol^{-1}; ref. 22).

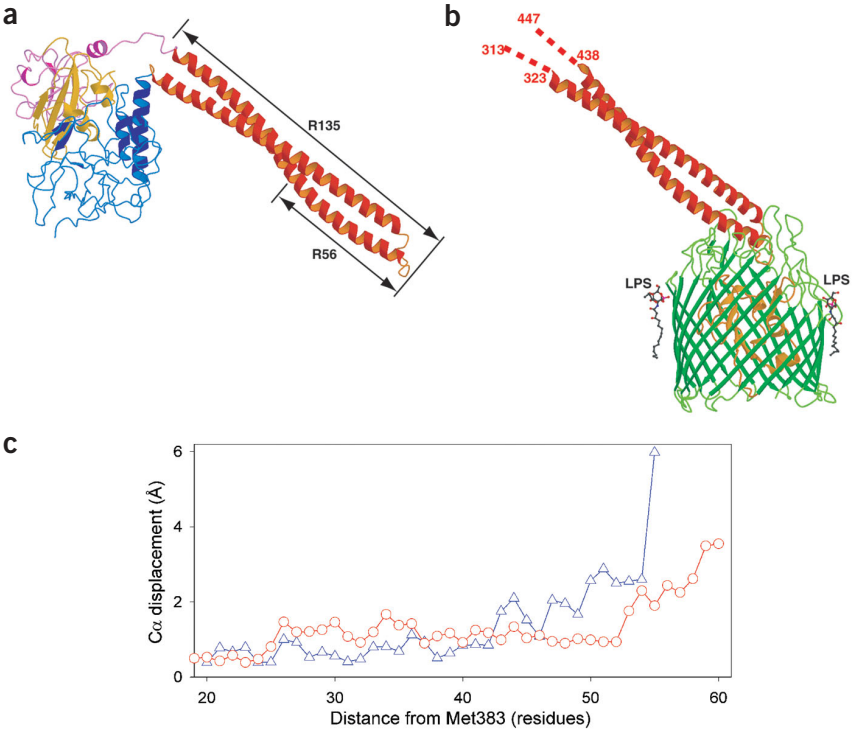

Figure 1 Structure of colicin E3 R-domain bound to BtuB. (**a**) The 551-residue colicin E3 (ribbon diagram) showing the extended coiled-coil segment that includes the receptor-binding (R) domain (red), N-terminal translocation (blue), C-terminal catalytic domain (magenta), and the bound immunity (Imm) protein (yellow)[10]. The R135 (Thr313–Glu447) and R56 (Lys355–Ala410) peptides are marked on the coiled-coil domain. (**b**) Structure of the complex between BtuB (barrel-cork in green-orange) and 116 residues (Y323–K438) of the 135-residue (Val316–Lys450) coiled-coil domain (red). Two molecules of LPS are seen and shown; seven bound LDAO molecules are not shown. Ten (Thr313–Asn322) N-terminal and nine (Lys439–Glu447) C-terminal residues (19/135 of total = 14%) of R135 were disordered upon binding and are not seen. (**c**) Conformational changes of bound R135. Displacement of α-carbon positions of R135 bound to BtuB relative to coordinates in the coiled coil of colicin E3 (ref. 10) Displacement is plotted as a function of distance, in residues, from Met383 at the apex of R135 as the origin. The coordinate displacement origin is defined by superposition of the BtuB-proximal 27 residues of R135 (**Fig. 1b**) with the same residues in colicin E3 (ref. 10). Red, Tyr323–Lys363; blue, Asp403–Lys438.

A shorter R56 peptide of colicin E3 binds somewhat more weakly to BtuB (K_d = 5.9 ± 1.1 nM; $k_a = 6.6 \pm 0.2 \times 10^5$ s^{-1} M^{-1}; $k_d = 3.8 \pm 0.6 \times 10^{-4}$ s^{-1}). The helical content of R56, detected by the decrease of molar ellipticity, increased from 31% to 67% upon binding to BtuB (**Fig. 2**). The entropy cost upon refolding R56 is presumably the cause of its weaker binding. The refolding upon binding to BtuB demonstrates a preference of the BtuB binding niche for the coiled-coil conformation.

A major finding of the present work is that only the region of the coiled coil near its tip is involved in binding to BtuB. The buried surface area of R135 bound to BtuB is 1,533 $Å^2$ or 24% of the coiled-coil domain of colicin E3 (R135), and 6.3% of the surface area of BtuB. The interaction surface between R135 and BtuB, defined by a 4.5-Å van der Waals distance of closest approach of residue atoms on R135 and BtuB, involves 27 residues of R135. This corresponds to one-fifth of the molecule, involving most of the resudues between Ile369 and Thr402. These residues interact with 29 residues of BtuB. R135 is bound mostly within the folded loop region of BtuB,

with the tip (Met383) of R135 extending to a quartet of residues, Thr55, Asn57, Leu63 and Ser64, at the top of the cork domain (**Fig. 3a**). Ten R135–BtuB residue pairs that interact closely (<3.4 Å) are (R135, BtuB): (Asn376, Tyr446), (His380, Asp448), (Asp381, Arg497), (Met383, Asn57), (Arg388, Tyr229), (Arg388, Leu240), (Trp390, Tyr405), (Gln398, Glu330), (Gln398, Tyr402) and (Thr402, Glu330). Of these residues in R135, the double mutant M383A W390A, causes a 10–50-fold decrease in colicin cytotoxicity, but the single mutants have no effect[10]. The mutant R399A of R135, which weakens binding to BtuB (data not shown), is within 3.7 Å of the acidic Glu330 of BtuB.

The structure of the BtuB–R135 complex also contains (i) the partial chain, including one sugar ring, of two bound lipopolysaccharide (LPS) molecules, one on each side of the structure (**Fig. 1b**) and (ii) seven molecules of the lauryl-dimethylamine-oxide (LDAO) detergent used for purification and crystallization (not shown). These molecules are bound to the exterior of the BtuB barrel, and may be part of a more complete detergent ring bound at the protein–detergent interface[23].

Although there are small conformational changes in the cork domain or β-strand region of BtuB caused by binding of R135, these changes cannot account for passage of the colicin polypeptide (**Fig. 3a**). Parameters that describe conformational change in the cork region caused by R135 binding are: (i) accessible surface area of the cork domain upon association with the barrel, which increases slightly upon binding (2,199 Å^2 versus 2,244 Å^2 for apo BtuB and R135–BtuB, respectively); (ii) number of barrel β-strands that interact with the cork (18 versus 16); (iii) number of hydrogen bonds between cork and barrel (60 versus 56); and (iv) in the TonB box on the periplasmic side of the cork domain[24], binding of R135 causes an ordering of the N-terminal Ser4-Pro5 residues of the box (**Fig. 3a**). These changes do not define a colicin import pathway through BtuB.

Five of the thirteen BtuB residues implicated in the binding of cobalamin[15], Tyr229, Asn276, Thr289, Arg497 and Tyr579 in the loop region, overlap the binding domain of R135 (**Figs. 3c,d**). The other eight residues that bind cobalamin but not R135 are located on the opposite side of the cobalamin (**Fig. 3d**). Overall, cobalamin is more deeply buried in BtuB. Only one of the BtuB residues utilized for Ca^{2+} binding[15], Tyr229, also interacts with R135. Ca^{2+} was not used during BtuB purification or in R135 binding solution, and was not detected in the R135–BtuB crystal structure.

Conformational changes in the extracellular loop region of BtuB

Binding of R135 to apo BtuB restores the order of loops 5–6 and 7–8 (2 of the 11 extracellular loops) that are disordered and not seen in the apo BtuB (**Fig. 3b**) structure. In addition, the position of loop 19–20 is changed and the location of the partial order in loop 3–4 is altered in R135–BtuB. There is a different pattern of loop order-disorder in the cobalamin–BtuB structure, where loops 3–4, 5–6 and 7–8 are reordered upon binding of the ligand, but loop 9–10 becomes disordered[15]. In FepA, conformational changes associated with the binding of colicin B have been detected in extracellular loop 5–6 (ref. 25).

A major problem addressed by the R135–BtuB structure is the pathway and mechanism of the translocation of colicin E3 across the outer membrane. A channel through the BtuB receptor would be a simple use of the receptor for translocation. However, the structure of BtuB, together with those of FepA, FhuA and FecA[16,18,26] implies that the N-terminal cork is firmly anchored to the β-barrel and occludes any large channel. Structurally defined conformational changes of the cork domain of FhuA accompany binding of ferrichrome ligand, but such changes are not sufficient to explain its transport[17]. These conformational changes are not sufficient to describe translocation of the 60-kDa colicin polypeptide, even when unfolded. However, formation

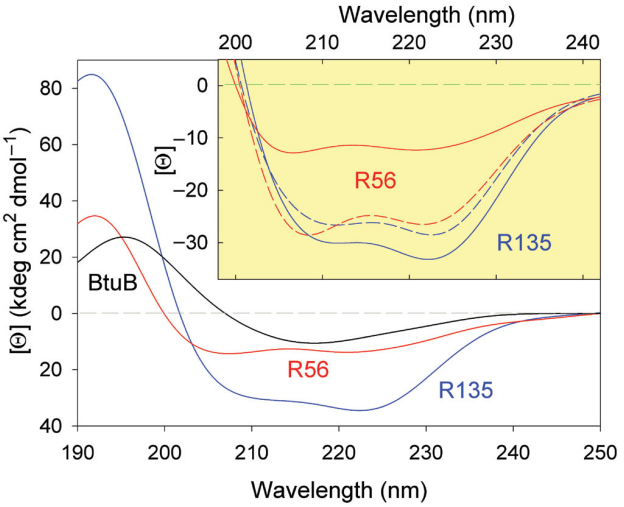

Figure 2 Secondary structure changes of R-peptides upon binding to BtuB. Far-UV CD spectra of R135 (blue), R56 (red) and BtuB (black) at 25 °C. α-Helical contents of R135 and R56 are 83 ± 5 (93) and 31 ± 4 (42)%, respectively. The helix content in parentheses is calculated without the N-terminal methionine, C-terminal $(His)_6$ and the eight residues of the apical loop and helical content of BtuB is <4% (ref. 15). Inset, CD spectra of R135 (blue) and R56 (red) in solution (solid), and bound to BtuB (dashed), were obtained by subtraction of the BtuB spectrum from that of the complex of R-peptide–BtuB. Change in number of residues in α-helix conformation upon binding to BtuB: R135, decrease from 118 ± 6 to 101 ± 3 residues; R56, increase from 20 ± 2 to 46 ± 4 residues.

in planar bilayers of large channels (~1 nS at 0.1 M ionic strength) by FhuA caused by addition of bacteriophage T5 suggested displacement of the cork and unmasking of an inner channel by the bound phage[27]. It has not been possible to observe such an effect caused by addition of colicin E3 to BtuB incorporated into planar bilayers and no significant channel activity is associated with BtuB (data not shown)[28]. The absence of significant BtuB channel activity implies that the peripheral and oblique binding of R135 to BtuB (**Fig. 1b**) does not characterize an intermediate in the insertion of colicin into BtuB. Rather, the function of peripheral binding of colicin E3 to BtuB is to initially concentrate the colicin on the membrane surface, changing the colicin diffusion from three to two dimensions. Through the extended coiled coil, the colicin E3–BtuB complex may subsequently function to contact a second outer-membrane protein that can act as a translocator[9]. Based on mutant analysis showing that the nuclease-E colicins and colicin A require the outer-membrane OmpF porin for cytotoxicity[29], the large ion channel conductance of OmpF[30], and its 7 × 11 Å channel cross-section that is sufficient for insertion of an unfolded polypeptide[31,32], it was hypothesized that the putative second receptor or translocator would be OmpF[33]. A role for OmpF in colicin E9 cytotoxicity has been shown in spot-test assays[34], although the activity of BtuB in these experiments was ~1/1,000 that in the present studies and in Taylor *et al*[19].

This hypothesis is supported in the present study by a specific occlusion of OmpF channels in planar bilayers by colicin E3 added to the *trans*-side (**Fig. 4a,b**) but not the *cis*-side (**Fig. 4b**) of the membrane bilayer; a requirement is shown for the presence of a *cis*-negative potential of ~50 mV (**Fig. 4a,b**), but no effect with a *cis*-positive potential (**Fig. 4a,b**). With *trans*-side colicin added in the presence of a *cis*-side negative potential, transient closing (flickering) of the channels was observed for ~10 s. Presumably, this shows the initial insertion

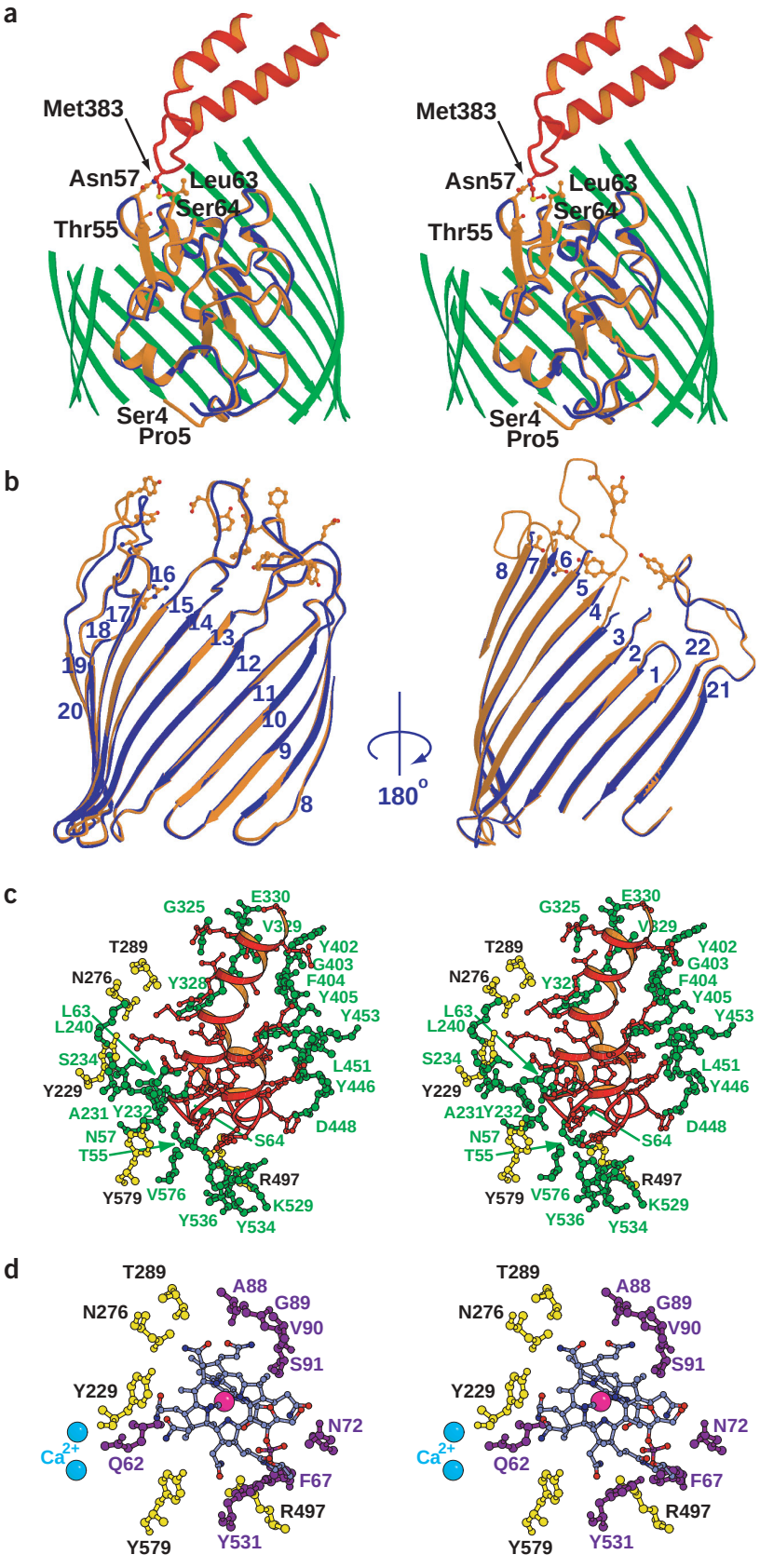

into the channels. Channel occlusion was essentially complete after 10 s (**Fig. 4b**). Channels stay blocked under *cis*-negative potentials. Closing of only one to two channels of the tripartite OmpF can be observed with a lower colicin concentration. Reversing the potential to *cis*-positive opened the occluded OmpF channels (data not shown). Colicin E1 or the colicin E3 R135 peptide added to the *trans*-side at a 100-fold greater concentration did not cause occlusion of the OmpF channels, although E1 occludes TolC channels (data not shown). The colicin occlusion effect is consistent with the *cis-trans* sides of the planar membrane being analogous to the periplasmic and extracellular sides of the outer membrane *in vivo*. The requirement of the *cis*-negative membrane potential implies that the *in vitro* occlusion occurs by electrophoretic insertion of part of the colicin. Occlusion was not observed when an excess of a proteolytic (thermolysin) fragment of colicin E3, from which the N-terminal 80 residues were removed, was added. This implies that the OmpF-recognition site is located in the glycine-rich disordered N-terminal segment of the T-domain.

DISCUSSION

The hypothesis for an interaction between BtuB and OmpF that would be mediated by the coiled coil bound to BtuB is described using a model of intact colicin E3 bound to BtuB (**Fig. 5**). The model shows the extrapolation of

Figure 3 Structure changes induced in BtuB by binding of R135 or cobalamin. (**a**) Changes in BtuB cork domain containing TonB site. The binding site of the receptor-proximal region of R135 (red) is superimposed on models of the cork region of apo BtuB (blue) and BtuB with bound R135 (orange). The staves of the BtuB β-barrel are green. The TonB box of BtuB is marked at the bottom by the N-terminal Ser4-Pro5 residues that are ordered upon R135 binding. (**b**) Changes in structures of barrel and loop domains of BtuB. Divided superimposed models of apo BtuB (blue) and R135–BtuB (orange). The barrel structure, with cork domain omitted, is divided for the sake of clarity; the left-hand panel is in the same orientation as **Figure 1b**, and the right-hand panel is rotated by 180°. The number of the β-strand in the barrel is shown. (**c**) Comparison of interaction between R135 or cobalamin and BtuB. Stereo views of the residues involved in interaction with R135 (red). The five BtuB residues used in complex formation with both R135 and cobalamin are yellow, and the BtuB residues used exclusively to bind R135 are green. (**d**) Stereo view of residues involved in interaction with cobalamin (light purple). The orientation is same as in **c**. The five residues that overlap with R135 binding are yellow and the eight used solely for cobalamin binding are purple.

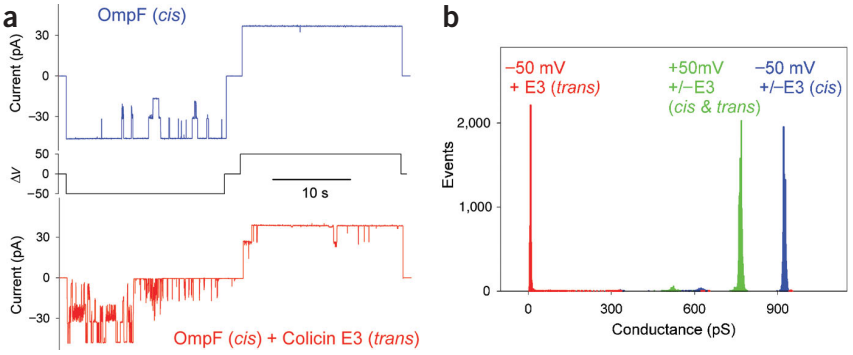

Figure 4 Occlusion by colicin E3 of OmpF incorporated into planar bilayers. (**a**) Transmembrane current across the planar bilayer with incorporated OmpF trimers in the absence (blue) or presence in the *trans*-compartment of colicin E3 (red) at a transmembrane potential of 50 mV. (**b**) OmpF channel conductance histogram for current in the absence or presence of colicin E3, recorded 10–30 s after the potential was applied. Trimer conductance: (i) ~900 pS with *cis*-negative potential in the absence of colicin, or colicin added to *cis*-side (blue histogram); (ii) 770 pS with *cis*-positive potential, in the absence of colicin, or in the presence of colicin added *trans*- or *cis*-side (green); (iii) occluded by colicin added to *trans*-side only with *cis*-negative potential in the presence of colicin (red). For conductance measurements, transmembrane current data measured 10–30 s after voltage application were used. Single-channel conductances of OmpF without colicin are 310 and 260 pS at –50 mV and +50 mV, respectively.

the structure shown in **Figure 1b** to the complete colicin E3 molecule[10]. Using the R135–BtuB structure, we predict that the binding of colicin E3 to BtuB will place the translocation domain close to the membrane surface, in a position where it can interact with another membrane protein, such as OmpF. Interaction with OmpF is made more likely by its large abundance, high surface density (~10^5 OmpF per cell; ref. 35; ~1 OmpF per 5,000 Å^2) and resulting close proximity (~50–100 Å). Such an interaction is made more likely by the conformational flexibility of (i) the disordered N-terminal domain of the colicin[36], (ii) the relatively weak binding of the T-domain to immunity protein discussed above[22] and (iii) the extended coiled coil, which would allow the colicin to 'scan' the membrane surface for the receptor binding site. In addition, the extended coiled coil shown in **Figures 1a,b** and **5** is very flexible. If it is assumed to be a cantilever with a Young's modulus for bending similar to that of other extended coiled-coil proteins[37], little more than thermal energy (~10^{-20} pN m) is required for small (~10°) angular deflections that would allow sampling of the surface of the membrane and of the OmpF population. Subsequent steps in the translocation process involve the interaction of the N-terminal segment of the colicin T-domain with the OmpF population, hypothetical threading of this segment through the OmpF channel, and interactions with the TolB and Pal components in the periplasm and peptidoblycan (PG) layer[7] (**Fig. 5**).

Initial threading of the colicin through the 7 × 11 Å aperture of OmpF[31,32] would not require a large energy input other than that needed for directionality because the T-domain is largely unfolded. No electron density is seen for the disordered[35] glycine-rich N-terminal 83 residues that contain the Asp35–Trp39 recognition site for the periplasmic TolB protein required for translocation[7]. Imm is sandwiched between the T- and C-domains, with 38% of its buried surface in contact with the T-domain[10]. The subsequent translocation events that release the tightly bound immunity protein before entry into the periplasm[8] and thereby trigger the unfolding necessary for entry of the C-terminal catalytic domain are unknown at present. They must be related to the driving force for translocation across the outer membrane and interaction with the periplasmic Tol proteins[7].

On the basis of the requirement of a membrane potential across the planar membrane bilayer for occlusion of the OmpF channels by colicin E3 (**Fig. 4a,b**), we propose that this potential constitutes part of the driving force. The existence of an electrical potential across the outer membrane *in vivo* has been debated in the literature[38,39]. It has been argued that the only potential that can exist across the outer membrane is a Donnan potential, which does not affect solute flow[39]. However, we note that the asymmetric outer membrane implies an asymmetry in the dipole potential that by itself would create a transmembrane potential[40].

METHODS

Purification and activity assay of colicin E3. The purification of colicin E3 was modified from an existing protocol[41]. The colicin was expressed in *E. coli* C43 (pcolE3) (C43 provided by J. Walker, Cambridge, UK) induced with mitomycin C. Crude colicin prepared by extraction from cells in high ionic strength and subsequent $(NH_4)_2SO_4$ precipitation was further purified on a DEAE-Sephadex A50 column. Colicin concentrations were determined using its extinction coefficient, ε (280 nm) = 79 cm^{-1} mM^{-1}. Colicin cytotoxicity was assayed by spot tests of the colicin added in a 15 µl aliquot on a lawn of sensitive *E. coli* cells K17 spread on Petri plates containing ampicillin (100 µg ml^{-1}).

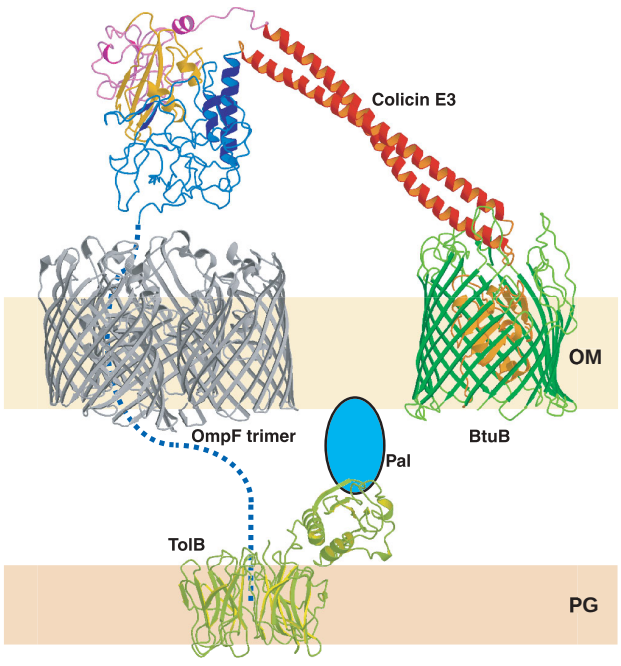

Figure 5 A model for a two-receptor translocon used for import of intact colicin E3. The colicin bound to BtuB shows the positions of the colicin translocation (blue), catalytic (magenta) and immunity (yellow) domains extrapolated from the structure of R135–BtuB (**Fig. 1b**), relative to a neighboring OmpF trimer in the outer membrane bilayer (OM). A collision with OmpF, hypothetical threading though OmpF of the colicin T-domain and subsequent interactions with the TolB and Pal components in the periplasm and peptidoglycan (PG) layer[7] are shown.

Table 1 Data collection and refinement statistics

Data collection	
Resolution range (Å)	35.5–2.75 (2.85–2.75)
R_{merge}[a,b]	0.084 (0.295)
Completeness[a]	96.7 (91.1)
$<I / \sigma I>$[a]	15.04 (2.90)
Number of reflections	
Total	139,699
Unique	37,175
Redundancy	3.8
Refinement	
R_{cryst}[c]	0.244
R_{free}[c]	0.293
R.m.s. deviations	
Bonds (Å)	0.016
Angles (°)	1.868
R.m.s. *B*-values (Å^2) (Bonds/angles)	
Main chain	0.50/0.97
Side chain	1.75/2.78
Mean *B*-values (Å^2)	33.3

[a]Values in parentheses apply to the highest-resolution shell. [b]$R_{merge} = \Sigma_h \Sigma_i | I_i(h) - <I(h)> | / \Sigma_h \Sigma_i I_i(h)$ where I_i is the i^{th} measurement of reflection h and $<I(h)>$ is a weighted mean of all measurements of h. [c]$R = \Sigma_h | F_{obs}(h) - F_{calc}(h) | / \Sigma_h | F_{obs} |$. R_{cryst} and R_{free} were calculated from the working and test reflection sets, respectively. The test set comprised 5% of the total reflections not used in refinement.

Purification of the colicin E3 coiled-coil domain (R135). The R135 coiled-coil domain and R56 were obtained using *E. coli* strain BL21 (DE3) for overexpression from plasmid pBluescriptKS (E3), cloned after *Nde*1 and *Xho*1 digestion into the vector pET21b, which has a strong T7 polymerase promoter and a C-terminal His_6-tag. For R135, this resulted in a 142-residue peptide, which includes 135 colicin E3 residues (Thr313–Glu447), an N-terminal methionine, and a C-terminal additional Glu-$(His)_6$ sequence. R135 with the $(His)_6$-tag was used in all experiments including for crystallization of R135–BtuB complex. The broken cell supernatant was purified by Ni-column chromatography (Novagen). R-peptide concentrations were determined using extinction coefficients from ε (280 nm) = 8.25 cm^{-1} mM^{-1} for R135, and 5.69 for R56 (residues 355–410).

Purification of BtuB. BtuB was expressed in strain TNEO12 (pJC3) and purified by a protocol similar to that described[19]. BtuB was extracted from outer membranes by 1.5% (w/v) β-D-octyl-glucoside, 50 mM Tris-HCl, 5 mM EDTA, PMSF/TPCK, pH 8.0, and purified by ion exchange chromatography in 0.1% (w/v) LDAO, using a 0–0.8 M LiCl gradient in a DEAE FPLC column. BtuB-enriched fractions were concentrated and further purified on Superdex 200HR in 10 mM Tris-HCl, 0.1 M NaCl, 0.1% (w/v) LDAO, pH 8.0. BtuB concentrations were determined from ε (280 nm) = 137 cm^{-1} mM^{-1}.

Activity of BtuB and R135 peptide. The activity of BtuB was assayed by its ability to neutralize the cytotoxicity of colicin E3 assayed by the microbiological spot test[19]. BtuB in detergent solution was mixed with the colicin at different molar ratios before addition of a small aliquot to the Petri plate. The activity of the R135 peptide was assayed by its ability to prevent colicin neutralization by BtuB by effectively competing for the colicin binding site on BtuB.

R-peptide–BtuB binding constants. Dissociation constants, K_d, of R-peptides with BtuB were determined by surface plasmon resonance from the association and dissociation rate constants of BtuB in detergent with surface-bound R-peptide using a Biacore 3000. R-peptide was bound to a CM5 (carboxymethylated dextran) chip using a sensor sandwich of His-tagged R-peptide bound to anti-His-tag monoclonal antibody (Novagen) that was immobilized in 10 mM sodium acetate, pH 4.0, on the chip, with a sandwich lacking antibody as the reference. R-peptide (0.5 μM) was injected at a flow rate of 5 μl min^{-1} (20 min) and washed for ≥5 min to reach a binding equilibrium, relative to which BtuB binding to R-peptide was measured. BtuB (0.13 μM) was added (20 min) at a flow rate of 5 μl min^{-1} in 10 mM Tris, 0.1 M NaCl, 0.1% (w/v) LDAO, pH 8.0. Dissociation was subsequently measured during flow of the same buffer without BtuB. No association or dissociation was observed when purified FepA receptor (from P. Klebba, University of Oklahoma, Norman, Oklahoma, USA) was added instead of BtuB. Qualitative determination of K_d values for the colicin and R-peptides was carried out by BtuB neutralization of colicin E3 cytotoxicity, and R-peptide neutralization of BtuB, as described above.

Circular dichroism spectroscopy. Far-UV CD measurements were carried out with a J-810 spectropolarimeter (JASCO) equipped with Peltier temperature control. Spectra were measured at 25 °C, using an optical path length, 0.1 mm, which minimizes spectral interference from buffer components. The data were plotted after application of the fast Fourier transform noise reduction algorithm. Molar ellipticity values at 222 nm were used to calculate helix content based on the theoretical value (–39,500 deg cm^2 dmol^{-1}; ref. 42) for a helix of infinite length. The secondary structure content of R-peptides in the presence of BtuB was derived from the difference spectrum of R-peptide bound to BtuB from which that of BtuB alone was subtracted. Buffer: 10 mM Tris-HCl, pH 8.0, 0.1 M NaCl, 0.1% (w/v) LDAO; temperature, 25 °C.

Planar bilayer measurements. Planar bilayer lipid membranes were formed using a 0.2-mm aperture in a teflon partition separating two compartments of the experimental cell from a 20 mg ml^{-1} solution of DOPC and DOPE (1:1) in *n*-decane. Only membranes with resistance higher than 100 GΩ were used. The aqueous solutions were buffered by 5 mM potassium phosphate, pH 7.0, 0.1 M KCl, 23 °C. OmpF (1–5 μl) was added from a 1.5 ng ml^{-1} stock solution containing 2% (w/v) octyl-glucoside. Colicin was added to the *cis*- or *trans*-side of the membrane. Membrane current was measured with a pair of Ag and AgCl electrodes connected to a Warner Instruments BC-525C amplifier. The potential was applied to the electrode on the *cis*-side of the membrane. Buffer: 5 mM potassium phosphate, pH 7.0, 0.1 M KCl. OmpF (0.3 pM) was added to the *cis*-side of the planar bilayer and magnetically stirred until channels were detected. To prevent incorporation of new OmpF channels, the *cis*-chamber was perfused before addition of colicin E3, 1.6 nM, into the *trans*- or *cis*-chamber.

Crystallization of the R135–BtuB complex. Crystallization was achieved in hanging drops at 20 °C using R135 and BtuB at a ratio (mol/mol) of 1.25:1 in 10 mM MES, pH 6.5, 0.1 M NaCl, 0.1% (w/v) LDAO, mixed 1:1 with a reservoir solution consisting of 0.1 M ADA buffer, pH 6.0, and 0.9 M $(NH_4)_2SO_4$. Crystals of the BtuB-R135 complex were visible after 2 weeks and reached a maximum size in ~2 months.

Structure determination and refinement. X-ray diffraction data summarized in **Table 1** were collected at a wavelength of 0.92 Å at beamline 19BM on the SBC-beam line (Advanced Photon Source, Argonne, Illinois, USA). Diffraction data to 2.75-Å resolution were collected at 100 K on a CCD-based SBC detector system, and were processed with the program HKL2000 (ref. 43). Crystals belong to orthorhombic space group $P2_12_12_1$, with unit-cell parameters $a = 76.93$, $b = 80.10$ and $c = 233.60$ Å. The calculated solvent content is 71.4% ($V_M = 4.3$ Å^3 Da^{-1}). The structure was determined by molecular replacement using AMoRe[44]. Apo BtuB coordinates (PDB entry 1NQE) were used as the search model. One BtuB–R135 complex in the asymmetric unit was refined with the program REFMAC5 in CCP4. **Figures 1a–c**, **3** and **5** that describe the structure information were drawn with BobScript[45] and Raster3D[46].

Coordinates. The atomic coordinates and structure factors have been deposited with the Protein Data Bank (accession code 1UJW).

Note: Supplementary information is available on the Nature Structural Biology website.

ACKNOWLEDGMENTS

We thank M. Lindeberg for experimental contributions in the early stages of these studies, J.T. Bolin, K. Jakes, and A. Raman for helpful discussions, P. Loll for samples of purified OmpF and W. Minor for generously sharing beam time. These studies have been supported by the US National Institutes of Health (NIH) and the Henry Koffler Professorship (WAC), a fellowship from the Japanese Ministry of Science and Education (G.K.), with NIH (M.W.), NIH/Fogarty (W.A.C. and Y.A.) and US Department of Energy and NIH National Center for Research Resources supporting, respectively, the Advanced Photon Source SBC-19BM and BioCARS 14-BMC beamlines. We thank R. Alkire, N. Duke, and G. Navrotski for assistance on the beamlines.

COMPETING INTERESTS STATEMENT

The authors declare that they have no competing financial interests.

Received 17 May; accepted 25 August 2003
Published online at http://www.nature.com/naturestructuralbiology/

1. Keenan, R.J., Freymann, D.M., Stroud, R.M. & Walter, P. The signal recognition particle. *Annu. Rev. Biochem.* **70**, 755–775 (2001).
2. Rehling, P. *et al.* Protein insertion into the mitochondrial inner membrane by a twin-pore translocase. *Science* **299**, 1747–1751 (2003).
3. Schwartz, T. & Blobel, G. Structural basis for the function of the β subunit of the eukaryotic signal recognition particle receptor. *Cell* **112**, 793–803 (2003).
4. Breyton, C., Haase, W., Rapoport, T.A., Kuehlbrandt, W. & Collinson, I. Three-dimensional structure of the bacterial protein-translocation complex SecYEG. *Nature* **418**, 662–665 (2002).
5. Braun, V. Energy-coupled transport and signal transduction through the gram-negative outer membrane via TonB-ExbB-ExbD-dependent receptor proteins. *FEMS Microbiol. Rev.* **16**, 295–307 (1995).
6. James, R., Penfold, C.N., Moore, G.R. & Kleanthous, C. Killing of *E. coli* cells by E group nuclease colicins. *Biochimie* **84**, 381–389 (2002).
7. Bouveret, E. *et al.* Analysis of the *Escherichia coli* Tol-Pal and TonB systems by periplasmic production of Tol, TonB, colicin, or phage capsid soluble domains. *Biochimie* **84**, 413–421 (2002).
8. de Zamaroczy, M. & Buckingham, R.H. Importation of nuclease colicins into *E. coli* cells: endoproteolytic cleavage and its prevention by the Immunity protein. *Biochimie* **84**, 423–432 (2002).
9. Cao, Z. & Klebba, P.E. Mechanisms of colicin binding and transport through outer membrane porins. *Biochimie* **84**, 399–412 (2002).
10. Soelaiman, S., Jakes, K., Wu, N., Li, C.M. & Shoham, M. Crystal structure of colicin E3: implications for cell entry and ribosome inactivation. *Mol. Cell* **8**, 1053–1062 (2001).
11. Gernert, K.M., Surles, M.C., Labean, T.H., Richardson, J.S. & Richardson, D.C. The alacoil: a very tight, antiparallel coiled-coil of helices. *Protein Sci.* **4**, 2252–2260 (1995).
12. Wiener, M., Freymann, D., Ghosh, P. & Stroud, R.M. Crystal structure of colicin Ia. *Nature* **385**, 461–464 (1997).
13. Di Masi, D.R., White, J.C., Schnaitman, C.A. & Bradbeer, C. Transport of vitamin B_{12} in *Escherichia coli*: common receptor sites for vitamin B_{12} and the E colicins on the outer membrane of the cell envelope. *J. Bacteriol.* **115**, 506–513 (1973).
14. Bradbeer, C., Woodrow, M.L. & Khalifah, L.I. Transport of vitamin B12 in *Escherichia coli*: common receptor system for vitamin B12 and bacteriophage BF23 on the outer membrane of the cell envelope. *J. Bacteriol.* **125**, 1032–1039 (1976).
15. Chimento, D.P., Mohanty, A.K., Kadner, R.J. & Wiener, M. Substrate-induced transmembrane signaling in the cobalamin transporter BtuB. *Nat. Struct. Biol.* **10**, 394–401 (2003).
16. Buchanan, S.K. *et al.* Crystal structure of the outer membrane active transporter FepA from *Escherichia coli*. *Nat. Struct. Biol.* **6**, 56–63 (1999).
17. Ferguson, A.D., Hofmann, E., Coulton, J.W., Diederichs, K. & Welte, W. Siderophore-mediated iron transport: crystal structure of FhuA with bound lipopolysaccharide. *Science* **282**, 2215–2220 (1998).
18. Ferguson, A.D. *et al.* Structural basis of gating by the outer membrane transporter FecA. *Science* **295**, 1715–1719 (2002).
19. Taylor, R., Burgner, J.W., Clifton, J. & Cramer, W.A. Purification and characterization of monomeric *Escherichia coli* vitamin B_{12} receptor with high affinity for colicin E3. *J. Biol. Chem.* **273**, 31113–31118 (1998).
20. Boetzel, R. *et al.* Structural dynamics of the receptor-binding domain of colicin E9. *Faraday Discuss. Chem. Soc.* **122**, 145–162 (2002).
21. Penfold, C.N. *et al.* A 76-residue polypeptide of colicin E9 confers receptor specificity and inhibits the growth of vitamin B12-dependent *Escherichia coli* 113/3 cells. *Mol. Microbiol.* **38**, 639–649 (2000).
22. Walker, D., Moore, G.R., James, R. & Kleanthous, C. Thermodynamic consequences of bipartite immunity protein binding to the ribosomal ribonuclease colicin E3. *Biochemistry* **42**, 4161–4171 (2003).
23. Prince, S.M. *et al.* Detergent structure in crystals of the integral membrane light-harvesting complex LH2 from *Rhodopseudomonas acidophila* strain 10050. *J. Mol. Biol.* **326**, 307–315 (2003).
24. Larsen, R.A., Thomas, M.G. & Postle, K. Protonmotive force, ExbB, and ligand-bound FepA drive conformational changes in TonB. *Mol. Microbiol.* **31**, 1809–1824 (1999).
25. Jiang, X. *et al.* Ligand-specific opening of a gated-porin channel in the outer membrane of living bacteria. *Science* **276**, 1261–1264 (1997).
26. Locher, K.P. *et al.* Transmembrane signaling across the ligand-gated FhuA receptor: crystal structures of free and ferrichrome-bound states reveal allosteric changes. *Cell* **95**, 771–778 (1998).
27. Plancon, L., Chami, M. & Letellier, L. Reconstitution of FhuA, an *Escherichia coli* outer membrane protein, into liposomes. Binding of phage T5 to FhuA triggers the transfer of DNA into the proteoliposomes. *J. Biol. Chem.* **272**, 16868–16872 (1997).
28. Eroukova, V.Y. *et al.* Occlusion of channel activity of secondary outer membrane receptors by colicins. *Biophys. J.* **84**, 521a (2003).
29. Benedetti, H. *et al.* Comparison of the uptake systems for the entry of various BtuB groups colicins into *Escherichia coli*. *J. Gen. Microbiol.* **135**, 3413–3420 (1989).
30. Schindler, H. & Rosenbusch, J.P. Matrix protein from *Escherichia coli* outer membranes forms voltage-controlled channels in lipid bilayers. *Proc. Natl. Acad. Sci. USA* **75**, 3751–3755 (1978).
31. Cowan, S.W. *et al.* Crystal structures explain functional properties of two *E. coli* porins. *Nature* **358**, 727–733 (1992).
32. Jeanteur, D. *et al.* Structural and functional alterations of a colicin-resistant mutant of OmpF porin from *Escherichia coli*. *Proc. Natl. Acad. Sci. USA* **91**, 10675–10679 (1994).
33. James, R., Kleanthous, C. & Moore, G.R. The biology of E colicins: paradigms and paradoxes. *Microbiology* **142**, 1569–1580 (1996).
34. Law, C.J. *et al.* OmpF enhances the ability of BtuB to protect susceptible *Escherichia coli* cells from colicin E9 cytotoxicity. *FEBS Lett.* **545**, 127–132 (2003).
35. Nikaido, H. & Vaara, M. In *Outer Membrane in Escherichia coli and Salmonella typhimurium* (ed. Neidhordt, F.C.) 7–22 (American Society of Microbiology, Washington, DC, 1987).
36. Collins, E.S. *et al.* Structural dynamics of the membrane translocation domain of colicin E9 and its interaction with TolB. *J. Mol. Biol.* **318**, 787–804 (2002).
37. Howard, J. Polymer mechanics. In *Mechanics of Motor Proteins and the Cytoskeleton* 99–116 (Sinauer, Sunderland, Massachusetts, USA, 2001).
38. Schindler, H. & Rosenbusch, J.P. Matrix protein in planar membranes: clusters of channels in a native environment and their functional reassembly. *Proc. Natl. Acad. Sci. USA* **78**, 2302–2306 (1981).
39. Sen, K., Hellman, J. & Nikaido, H. Porin channels in intact cells of *Escherichia coli* are not affected by Donnan potentials across the outer membrane. *J. Biol. Chem.* **263**, 1182–1187 (1988).
40. Seydel, U., Eberstein, W., Schroder, G. & Brandenburg, K. Electrostatic potential in asymmetric planar lipopolysaccharide/phospholipid bilayers probed with the valinomycin-K^+ complex. *Z. Naturforsch. B* **47c**, 757–761 (1992).
41. Herschman, H.R. & Helinski, D.R. Purification and characterization of colicin E2 and colicin E3. *J. Biol. Chem.* **242**, 5360–5368 (1967).
42. Chen, Y.H., Yang, J.T. & Chau, K.H. Determination of the helix and β form of proteins in aqueous solution by circular dichroism. *Biochemistry* **13**, 3350–3359 (1972).
43. Otwinowski, Z. & Minor, W. Processing of X-ray diffraction data collected in oscillation mode. *Methods Enzymol.* **276**, 307–326 (1997).
44. Collaborative Computational Project, Number 4. The CCP4 suite: programs for protein crystallography. *Acta Crystallogr. D* **50**, 760–763 (1994).
45. Esnouf, R.M. An extensively modified version of MolScript that includes greatly enhanced coloring capabilities. *J. Mol. Graph.* **15**, 132–134 (1997).
46. Merritt, E.A. & Bacon, D.J. Raster3D: photorealistic molecular graphics. *Methods Enzymol.* **277**, 505–524 (1997).